INVESTIGATIONS OF $NiFe_{2-t}Al_tO_4$ SERIES BY ^{57}Fe AND ^{61}Ni MÖSSBAUER SPECTROSCOPY

J.J. Bara, Z.M. Stadnik
Institute of Physics, Jagiellonian University
Reymonta 4, 30-059 Cracow, Poland

G. Czjzek, J. Fink, V. Oestreich, H. Schmidt
Kernforschungszentrum Karlsruhe
Institut für Angewandte Kernphysik
D-7500 Karlsruhe, Postfach 3640, F.R.G.

The magnetic properties of ferrimagnets are determined by the type of ordering and strength of couplings of their magnetic atoms. The saturation magnetization and the Curie temperature obtained from magnetometric measurements are usually treated as characteristic parameters of a sample under investigation /1/. This is certainly correct for concentrated ferrimagnets, however, it may be not so for diluted ones, particularly at elevated temperatures. Diluted ferrimagnets are not homogeneous as far as the strength of magnetic couplings between ions is considered. This is due to the random distribution of non-magnetic atoms inside a given type of crystallographic position.

A bulk material is often considered to be divided into small regions of which the dimensions are widely varying throughout the crystal /2/. Magnetic ordering exists within these regions, whereas the magnetic interactions between neighbouring regions are supposed to be rather small, depending on the degree of dilution. There are thermally activated fluctuations of magnetic moments within regions and/or fluctuations of magnetization vectors of the regions, which are usually described in terms of magnetic /3-5/ or superparamagnetic /6-8/ relaxation processes. They cause the saturation magnetization of a sample and consequently its Curie temperature to be, from the microscopic point of view, time dependent functions. Thus, the experimentally determined saturation magnetization and Curie temperature are values averaged not only over the volume of the sample but also over the time interval of the measurement. Particularly this is the case for a magnetometric method, because it is a macroscopic method with the observation time of the order at least a few seconds. Magnetometric measurements are performed for external magnetic fields usually of the order of up to about 100 kOe. Such fields have strong influence on the rate of magnetic or superparamagnetic relaxation processes. Moreover, the application of high external magnetic fields may even change the ordering of ionic magnetic moments in ferrimagnets /9,10/, similarly as is observed in antiferromagnets /11,12/. Thus, the values of saturation magnetization and Curie temperature determined for diluted ferrimagnets by means of the magnetometric method may not necessarily have the same physical meaning as those determined for concentrated ferrimagnets. Comparison of the results obtained for diluted ferrimagnets by the magnetometric

method with those resulting from complementary methods are therefore of great importance.

The Mössbauer spectroscopy has proved to be a very good microscopic tool for studying the properties of diluted ferrimagnets /13,14/. This is due to its high energy resolution and short observation time. The ^{57}Fe Mössbauer spectroscopy can, for example, resolve two Zeeman patterns originating from hyperfine magnetic fields which differ by about 6 kOe. Thus, in contrast to the magnetometric method, Mössbauer spectroscopy is used for studying sublattice magnetizations /15/, and even their structure caused by the random distribution of non-magnetic atoms /16-19/. Such investigations do not require the application of external magnetic fields. However, if the external magnetic field is used its influence on the sublattice hyperfine fields can be directly observed. Moreover, the Mössbauer spectroscopy can register the fluctuation of hyperfine fields provided that its rate is of the order of the Larmor frequency /about 10^8 Hz for ^{57}Fe/ of a nuclear magnetic moment.

Diluted ferrimagnets often show Mössbauer spectra with shapes strongly dependent on temperature and on applied external magnetic field. Such behaviour is explained either by a random distribution of non-magnetic atoms and/or by relaxations of the magnetic or superparamagnetic type. Nickel ferrite-aluminates $NiFe_{2-t}Al_tO_4$ /$0<t<2$/ are good representatives of diluted ferrimagnets since non-magnetic Al^{3+} ions enter both the tetrahedral /A/ and the octahedral /B/ sites /20/.

In this paper we report some new results of ^{57}Fe and ^{61}Ni Mössbauer effect investigations of $NiFe_{2-t}Al_tO_4$ series performed in a wide temperature range and in high external magnetic fields. The results of our earlier studies have been published elsewhere /21/. In the present study special attention has been paid to the influence of temperature and external magnetic field on the shape of the Mössbauer absorption spectra. The ^{57}Fe measurements have been performed for the $t = 0.2$, 0.75, 1.0, 1.25, 1.3, 1.35, 1.5, 1.75 and 1.9 samples in a temperature range from 4.2 K to temperatures above appropriate Curie temperatures. For the $t = 1.25$ sample additional ^{57}Fe spectra have been taken at 301 K in the transverse external magnetic fields of 1 kOe and 4 kOe, while the $t = 1.5$ sample has been measured at 4.2 K in the longitudinal external magnetic field of 60 kOe. The ^{61}Ni measurements at 4.2 K have been done for the $t = 0.2$, 1.0, 1.5 and 1.9 samples. For the $t = 1.0$ and 1.9 samples additional ^{61}Ni spectra have been obtained at 4.2 K in $H_{ext} = 60$ kOe parallel to the gamma-ray direction. Some typical ^{57}Fe Mössbauer spectra of weakly /$t = 0.2$/ and highly /$t = 1.5$/ diluted samples are shown in Figs. 1 and 2, respectively.

Low temperature ^{57}Fe spectra of all the investigated samples are interpreted as composed of tetrahedral and octahedral Zeeman patterns. The influence of the random distribution of Al^{3+}, Ni^{2+} and Fe^{3+} ions in the A and B sublattices on the internal magnetic fields H/A/ and H/B/ corresponding to A and B sites, manifests itself as the broadening of Zeeman components. The observed Zeeman patterns are treated as not influenced by relaxation processes as long as the ratio $r_1 = \Delta_{16}/\Delta_{34}$ (or $r_2 = \Delta_{25}/\Delta_{34}$) is temperature independent; Δ_{ij} denotes the distance on the velocity scale between the i-th and j-th Zeeman line. The

values of r_1 and r_2 for static Zeeman patterns are 6.33 and 3.67, respectively. The above procedure is justified since the spectra exhibiting Zeeman patterns show no apparent quadrupole interaction. It is also the case for most investigated hitherto diluted spinels. This fact can be explained by taking into account the directions of easy magnetization and of the EFG principal axes /22/.

At elevated temperatures relaxation processes begin to play

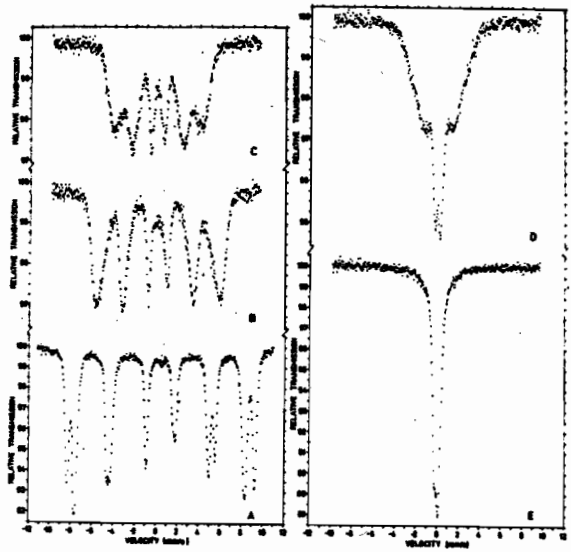

Fig. 1. ^{57}Fe Mössbauer spectra of $NiFe_{1.8}Al_{0.2}O_4$ at the temperatures of: A - 77 K, B - 601 K, C - 700 K, D - 750 K, E - 770 K.

an important role. They appear at lower temperatures for highly diluted samples than for weakly diluted ones. This is reflected in the Mössbauer spectra in the form of Zeeman line broadenings, larger than the broadening at low temperatures /Figs. 1 and 2/, and in a distinct increase in the values of r_1 and r_2 /Figs. 3, 4/.

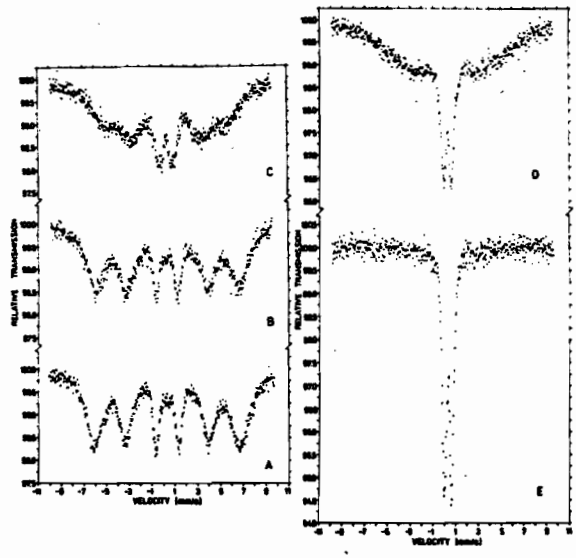

Fig. 2. ^{57}Fe Mössbauer spectra of $NiFe_{0.5}Al_{1.5}O_4$ at the temperatures of: A - 82 K, B - 92 K, C - 138 K, D - 162 K, E - 185 K.

The magnetic relaxation Mössbauer spectra are characterized by rather narrow and intense inner lines as compared with the broad outer ones. The growth of the inner lines at the expense of the outer ones is observed as temperature increases. The inner lines are the part of the relaxation Zeeman pattern and can not be treated as the superparamagnetic doublet originating from the superparamagnetic clusters /23/, unless the distinct structure of the inner lines can be clearly seen /24/. The shape of the relaxation spectrum changes in an applied external magnetic field, even of the order of a few kOe /Fig. 5/. The described

influence of temperature and of a relatively weak external magnetic field on the shape of the Mössbauer spectra is treated as evidence of the existence of relaxation processes of the magnetic type in the investigated series.

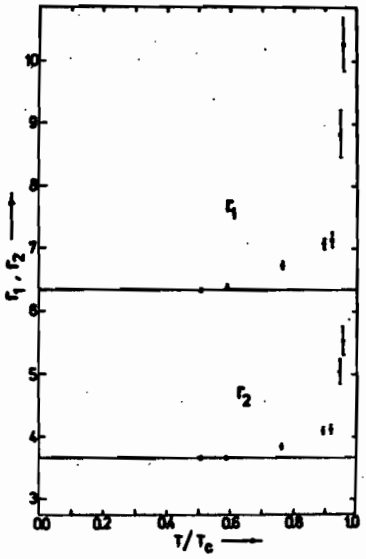

Fig. 3. r_1 /•/ and r_2 /o/ versus reduced temperature T/T_c for $NiFe_{1.8}Al_{0.2}O_4$.

A relaxation spectrum is fully transformed into a quadrupole doublet at the temperature above which the separation of the inner lines Δ_{34} is found to be only slightly dependent on the temperature /Fig. 6/. Some Mössbauer absorption spectra of each of the investigated samples show relaxation features over some temperature regions below its Curie temperature. These regions are narrow for weakly diluted samples and relatively wide for highly diluted ones. This is clearly seen in Fig. 7, in which three temperature regions A, B and C are distinguished. In region A normal /static/ Zeeman patterns are observed. Relaxation Mössbauer spectra are found in region B, while in region C quadrupole doublets are registered. For each of the investigated samples a quadrupole doublet is observed below the magnetometric Curie temperature. Similar behaviour was reported for the other ferrimagnets /2,8,25,26/. This seems to be clear evidence of the influence of the external magnetic field on the results derived from magnetometric measurements. For concentrated ferrimagnets this influence is removed by the extrapolation of saturation magnetization values, for a given temperature, to zero external magnetic field. However, this can not be correctly done for diluted ferrimagnets since their magnetic properties, investigated in an external magnetic field, strongly depend on the value of the field's strength and are distinctly different from those in a zero external magnetic field. This fact is due particularly to the stabilization of relaxation processes by the applied external magnetic field.

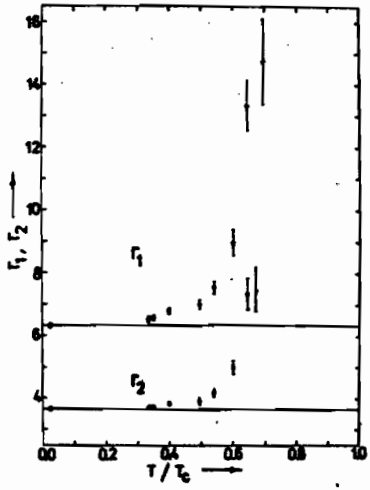

Fig. 4. r_1 /•/ and r_2 /o/ versus reduced temperature T/T_c for $NiFe_{0.5}Al_{1.5}O_4$.

The broadening of time-independent Zeeman spectra /region A in Fig. 7/ can be explained by a random distribution of Fe^{3+}, Ni^{2+} and Al^{3+} cations in the tetra-

hedral and in the octahedral sublattices. A tetrahedral ion has twelve nearest--neighbour B-site ions and four nearest-neighbour A-site ions, while an octahedral ion has six nearest-neighbour A-site ions and six nearest-neighbour B-site ions /27/. The distribution of Fe^{3+}, Ni^{2+} and Al^{3+} ions between the A- and B-sites has been determined previously /20,21/. Taking it into account, the probabilities of various possible nearest-neighbour B or A, or B and A, type configurations around a given tetrahedral or octahedral site ion can be calculated from the well known bionomial formula, assuming a statistical distribution of the ions in the tetrahedral and octahedral sublattices. In principle one Zeeman spectrum may be attributed to each of the nearest-neighbour configurations around the ferric ion in

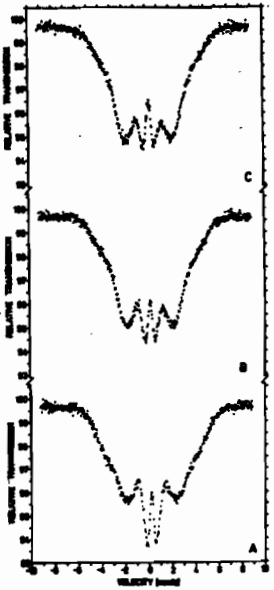

Fig. 5. ^{57}Fe Mössbauer spectra of $NiFe_{0.75}Al_{1.25}$ at 301 K when the transverse external magnetic field H_{ext} = 0 /A/, H_{ext} = 1 kOe /B/ and H_{ext} = 4 kOe /C/.

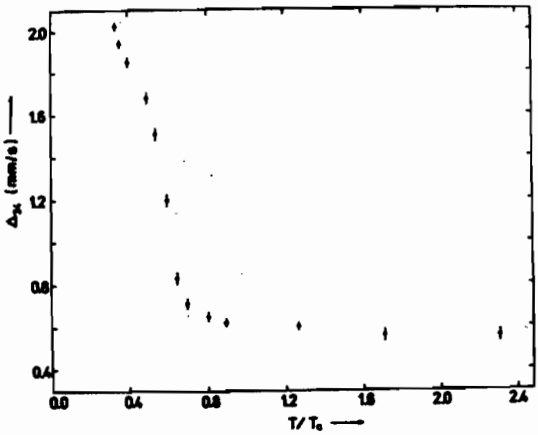

the A or B site. In order to explain the influence of the random distribution of Fe^{3+}, Ni^{2+} and Al^{3+} ions on the hyperfine magnetic fields H/A/ and H/B/ acting on ^{57}Fe nuclei at the A and B positions, respectively, one has to consider the strength of all

Fig. 6. Separation between innermost lines Δ_{34} versus reduced temperature T/T_c for $NiFe_{0.5}Al_{1.5}O_4$.

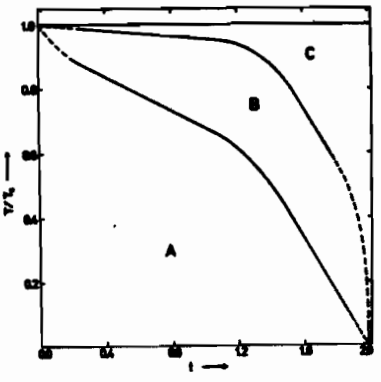

Fig. 7. The diagram of the types of Mössbauer spectra for the $NiFe_{2-t}Al_tO_4$ series. Three temperature regions are distinguished: A - time-independent Zeeman patterns region, B - relaxation region and C - quadrupole doublets region. The dashed lines indicate extrapolation.

couplings between magnetic ions. In most of the Mössbauer effect investigations of spinels performed hitherto, it was usually assumed that A-A and B-B couplings are negligible when compared with a strong A-B coupling. This is not the case for the $NiFe_{2-t}Al_tO_4$ series, since besides antiferromagnetic Fe/A/-Fe/B/ and Fe/A/-Ni/B/ couplings, also the ferromagnetic Fe/B/-Ni/B/ coupling of comparable strength, exists /1/. This was at least numerically verified for the t = 0.0 sample /15,28/.

It is a well established fact in the Mössbauer spectroscopy of spinels that the distribution of H/B/ is much larger than that of H/A/ /14,25,29,30/. This is also observed in the investigated series. Therefore, one H/A/ value is used in a fitting procedure. The small distribution of H/A/ values is included in linewidths of the Zeeman pattern corresponding to the A sublattice. The distribution of H/B/ values is caused by the weakening of Fe/A/-Fe/B/, Fe/A/-Ni/B/ and Fe/B/-Ni/B/ couplings when the samples are diluted with Al atoms. For a given nearest-neighbour configuration of the A and B type ions around the octahedral ferric ion, the hyperfine magnetic field acting on ^{57}Fe nuclei at the B positions may be approximated by the formula:

$$H_B(k,l,m,n) = H_B(0) + k\Delta H_1 + l\Delta H_2 + m\Delta H_3 + n\Delta H_4 ,$$

where $H_B(0)$ is the hyperfine field at the B site corresponding to the nickel ferrite /t = 0.0/ configuration, while $k\Delta H_1$, $l\Delta H_2$ and $m\Delta H_3$ characterize changes of H/B/ when k Fe/A/, l Fe/B/ and m Ni/B/ atoms are replaced by k, l and m Al atoms, respectively; $n\Delta H_4$ accounts for the replacements of n Fe/A/ atoms by n Ni/A/ ones. Each set of k, l, m and n integers corresponds to a given configuration of nearest-neighbour A- and B-site ions around an octahedral ferric ion. The sum of probabilities of configurations which are taken into account in the $H_B(k,l,m,n)$ fitting procedure is close to unity. The area under a Zeeman pattern corresponding to a given configuration is proportional to the probability of that configuration. The quadrupole interaction is assumed to be zero, both for the A and B sublattices. Three linewidths and one isomer shift are used as fit parameters for all B-site Zeeman patterns. Fig. 8 shows, as an example, the spectrum of the t = 0.2 sample at 404 K fitted with one A-site and twenty five B-site Zeeman patterns. The procedure for deriving ΔH_1 values from the fitted spectra, which is in progress, will make it possible to investigate the changes in ΔH_1 parameters with temperature and concentration of Al atoms. These parameters are very important since they characterize the supertransferred hyperfine fields in the investigated series /25,31,32/.

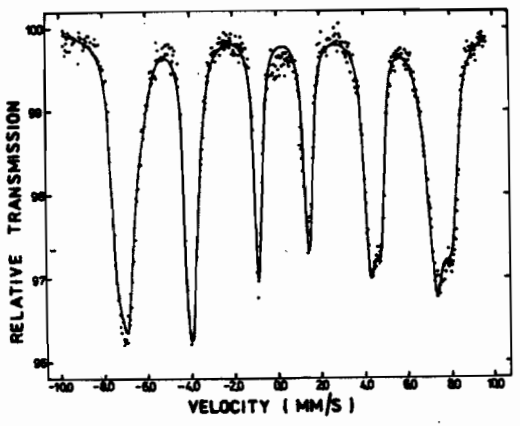

Fig. 8. ^{57}Fe Mössbauer spectrum of $NiFe_{1.8}Al_{0.2}O_4$ at 404 K. The solid line is a fit according to a procedure described in the text.

The Van Der Woude - Dekker description of the magnetic relaxation in Mössbauer spectra /3/ is being adopted for our spectra from the region B /Fig. 7/. We hope to obtain some information on the influence of temperature and sample dilution on the relaxation time.

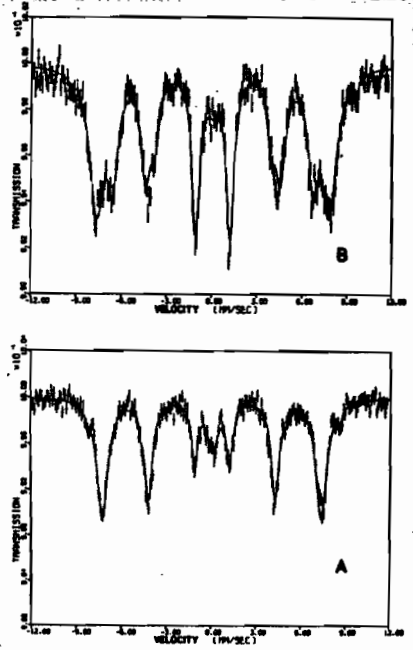

The ^{57}Fe spectra of the t = 1.5 sample measured at 4.2 K in zero and 60 kOe longitudinal magnetic field /Fig. 9/ show several interesting features. The spectrum in Fig. 9A is decomposed into three, while that in Fig. 9B - into four components /Table I/. Component I of the zero external magnetic field spectrum is the most intense one. It is concluded from its intensity and linewidth that both tetrahedral and octahedral Zeeman patterns are contained in this component. In order to elucidate on the broadening of the spectrum lines the fitting procedure for spectra from the temperature region A in Fig. 7, described above, is to be used.

Fig. 9. ^{57}Fe Mössbauer spectra of $NiFe_{0.5}Al_{1.5}O_4$ at 4.2 K in a zero external magnetic field /A/ and in a longitudinal field of 60 kOe /B/.

Table I. Results of data analyses by the transmission integral method based on the zero-field spectrum in Fig. 9A and on the applied-field spectrum in Fig. 9B. Notations used: c - fraction of the total intensity of a component /derived from areas/, δ - isomer shift with respect to pure Fe at 4.2 K, u - unpolarized fraction; γ and $M_2(H)$ refer to absorber widths /see ref. /33//. Values marked with * were kept constant during the fit. Standard deviations are given in parentheses.

/A/ H_{ext} = 0

Component	c(%)	δ (mm/s)	$\langle H_{hf} \rangle$ (kOe)	γ (mm/s)	$\sqrt{M_2(H)}$ (kOe)
I	86(2)	0.215(0.006)	452.9(0.5)	0.35(0.04)	14.7(0.8)
II	4(2)	0.35(0.03)	522(2)	0.1*	0*
III	10(2)	0.25(0.02)	0	0.72(0.09)	-

/B/ H_{ext} = 60 kOe

Component	c(%)	δ (mm/s)	$\langle H_{hf} \rangle$ (kOe)	γ (mm/s)	$\sqrt{M_2(H)}$ (kOe)	u
Ia	55(2)	0.213(0.009)	478(1.4)	0.35*	22.8(1.4)	0.84(0.03)
Ib	27(2)	0.213(0.009)	412.1(1.3)	0.35*	11.5(2)	0.76(0.06)
II	2(1)	0.35*	585(3)	0.1*	0*	0*
III	16(2)	0.25(0.05)	65(2)	0.7*	0*	0*

Component II comes from those B-site ferric ions whose nearest-neighbour coordination shell is more rich in Fe and Ni atoms than on the average. It is to be noted that such a component is observed throughout the whole composition range /$0 < t < 2$/ and its intensity decreases with dilution t, as should be expected. The component III is situated near zero velocity. It may come from Fe atoms which have been excluded from magnetic ordering due to the high Al dilution of the t = 1.5 sample or/and from Fe impurities in the berylium sample holder. The very weak /of the order of 1 % of the total intensity/ non-magnetic component is also indicated in the ^{61}Ni spectrum of this sample. The above mentioned alternative is to be solved in the following experiments. The external magnetic field increases the Zeeman splitting of component II by a value directly corresponding to H_{ext} = 60 kOe and induces a Zeeman splitting of non-magnetic component III. Component I is split into two parts Ia and Ib.

As is known from our magnetometric data /Fig. 6 in ref. 21/ the saturation magnetic moment per molecule has a negative value for samples with $0.63 < t < 1.6$. Therefore, the A sublattice magnetization is parallel, while the B sublattice magnetization is antiparallel to the external magnetic field vector, provided that collinear ordering of atomic magnetic moments exists. The collinear ordering has been proved for samples with $t \leqslant 1.25$ by our magnetometric and neutron diffraction measurements /21/. In a collinearly ordered sample from the $0.63 < t < 1.6$ region, with domains aligned parallel to the external magnetic field vector, the value of H_{ext} should be added to the H/B/ value. This is exactly the case for component II of the H_{ext} = 60 kOe spectrum. Thus, at least component II corresponds to iron B sites in which iron magnetic moments are collinearly ordered and aligned antiparallel to the external magnetic field vector.

The non-zero intensity of $\Delta m = 0$ lines of components Ia and Ib /Fig. 9B/ is certainly direct evidence that iron magnetic moments are not aligned parallel to the hyperfine magnetic field direction. However, this need not be necessarily treated as a proof of the non-collinear ordering of the t = 1.5 sample. Since the component II has been shown to be assigned to such B-site positions which are occupied by iron atoms with collinearly aligned magnetic moments, it is rather unlikely that non-collinearity will occur for iron atoms with a nearest-neighbour shell less rich in magnetic atoms. The dilution process, which effects both the A and B sublattices /21/, diminishes all inter- and intrasublattice magnetic couplings, probably without any distinct preference. The composition t = 1.5 is very near the compensation point composition /t = 1.6/, i.e. for the t = 1.5 sample the A sublattice magnetization only slightly surpasses the B sublattice magnetization. A small external magnetic field of the order of a few kOe will cause partial alignment of magnetic domains, if a collinear ordering of the sample is assumed. The A-site magnetization will be approximately parallel, while the B-site magnetization will be approximately antiparallel to the external magnetic field vector. Therefore, the A-site magnetization will be in an equilibrium energy state, but the B-site magnetization will not. An increase in the value of H_{ext} will "bend" the antiferromagnetic coupling between the A and B sublattice magnetizations /9,11,34/. The magnetic moment vectors of the A and B sublattices /$\vec{m}_A$ and $\vec{m}_B$/ will make the angles α_A and $180 - \alpha_B$ with $\vec{H}_{ext}$, respectively /Fig. 10/. α_B is larger than α_A since $m_A > m_B$. If a sample is con-

sidered as composed of small regions with various cation environments around the A and B sites, then the wide distribution of the α'_A and α'_B angles, now describing the directions of A and B magnetic moments in these regions relative to $\vec{H}_{ext}$, is expected. The resulting magnetic moment of a given region $\vec{m}' = \vec{m}'_A + \vec{m}'_B$ and the angles α'_A and α'_B depend on the strength of the applied magnetic field. The observed effective hyperfine magnetic field $\vec{H}_{hf}$ in a given crystallographic position is the vector sum $\vec{H}_{hf} = \vec{H}_o + \vec{H}_{ext}$ of the hyperfine field $\vec{H}_o$, as observed in this position in zero applied field, and the applied external magnetic field $\vec{H}_{ext}$. When $H_o \gg H_{ext}$ then the angles α'_A and α'_B close to 90 degrees will give H_{hf} values not much different from H_o, while those close

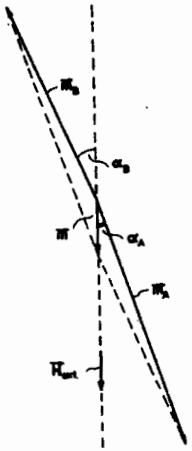

Fig. 10. The orientation of tetrahedral and octahedral magnetization vectors relative to $\vec{H}_{ext}$ vector.

to 0 degrees will give two well resolved Zeeman patterns. Intermediate situations are to be also considered while fitting the measured spectrum. The assumption of non-collinear ordering of the t = 1.5 sample has not given a satisfactory fit /solid line in Fig. 9B/ of the components Ia and Ib even when a large portion of non-polarized magnetic domains was taken into account. The spectrum in Fig. 9B appears to be explained by the influence of H_{ext} on the A and B magnetization vectors, as discussed above. In order to prove this interpretation, Mössbauer spectra are to be taken at 4.2 K in various external magnetic fields. The influence of H_{ext} on the shape of Mössbauer spectra, as reported in /10/, is supposed to be explained by the interpretation discussed above.

The results derived from ^{61}Ni Mössbauer spectra /Figs. 11-13/ are compiled in Table II. For the t = 0.2 and 1.0 samples Ni atoms were assumed to occupy only the B sites, while for the t = 1.5 and 1.9 samples the occupation of both the A and B positions by Ni atoms was taken into account in a fitting procedure.

Table II. Results of data analyses based on the ^{61}Ni spectra in Figs. 11-13. The symbols are the same as those used in Table I.

t	H_{ext}(kOe)	|H(B)| (kOe)	$\sqrt{M_2(H(B))}$ (kOe)	|H(A)| (kOe)	$\sqrt{M_2(H(A))}$ (kOe)
0.2	0	94.5(0.9)	6.7(0.2)		
1.0	0	99.1(0.2)	5.1(0.3)		
	60	161(2)	5.8(0.4)		
1.5	0	84.6(0.2)	7.2(0.4)	101.9(1.3)	0
1.9	0	68.2(0.3)	9.4(0.4)	87.0(1.3)	0
	60	59.7(0.3)	22.6(0.5)	111.4(0.9)	0

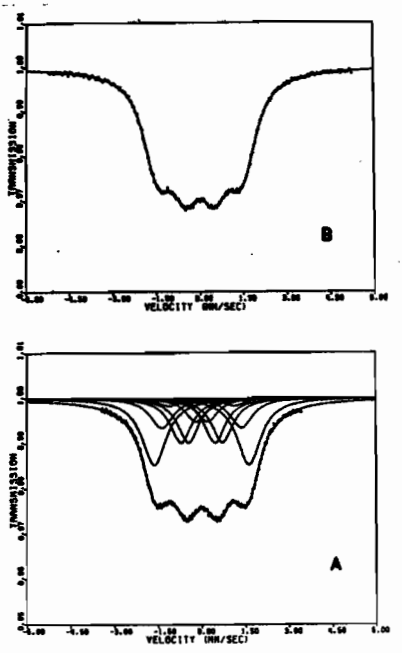

Fig. 11. ^{61}Ni spectra at 4.2 K of $NiFe_{1.8}Al_{0.2}O_4$ /A/ and $NiFe_{0.5}Al_{1.5}O_4$ /B/.

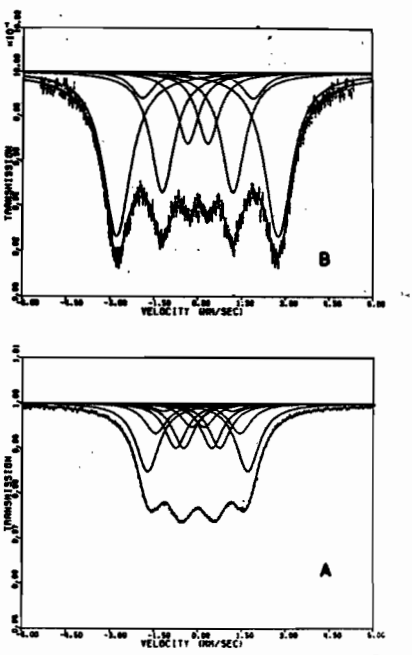

Fig. 12. ^{61}Ni spectra at 4.2 K of $NiFeAlO_4$ in zero external magnetic field /A/ and in a longitudinal external magnetic field of 60 kOe /B/.

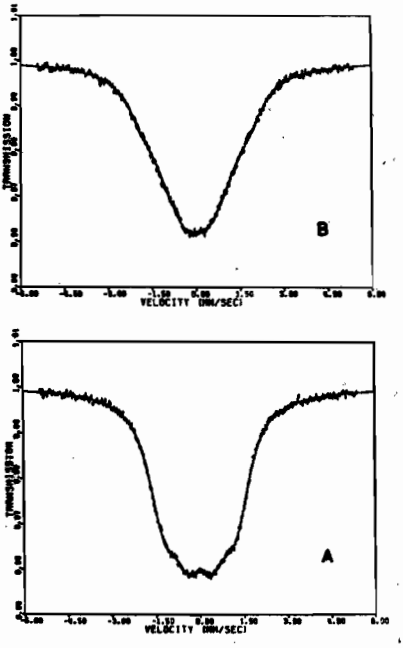

The hyperfine magnetic fields acting on ^{61}Ni nuclei at the B sites H/B/ were found to have values similar to those observed for other spinels /35/. They are smaller as compared with A-site hyperfine fields H/A/, which however are not so great as those reported in the literature /35/. Both fields decrease with dilution t, the B-site hyperfine fields faster than the A-site ones. The collinear ordering of magnetic moments for the t = 1.0 sample was shown by taking a ^{61}Ni spectrum at 4.2 K in the longitudinal external magnetic field H_{ext} = 60 kOe /Fig. 12B/. This spectrum is interpreted as being due to Ni atoms occupying only the B positions with mag-

Fig. 13. ^{61}Ni spectra at 4.2 K of $NiFe_{0.1}Al_{1.9}O_4$ in zero external magnetic field /A/ and in a longitudinal external magnetic field of 60 kOe /B/.

netic moments aligned antiparallel to the external magnetic field vector. The H_{ext} value was found to be added to the B-site hyperfine field value and it means that the sign of the B-site hyperfine field is negative. The ^{61}Ni Mössbauer spectrum of the t = 1.9 sample measured in H_{ext} = 60 kOe /Fig. 13B/ has a peculiar shape which can not be well fitted assuming a collinear alignment of Ni magnetic moments parallel to the external magnetic field vector. It may reflect the influence of H_{ext} on the ordering of the A and B sublattice magnetizations, as has been discussed earlier for the ^{57}Fe spectrum of the t = 1.5 sample measured in H_{ext} = 60 kOe. The comparison of spectra in Fig. 13 shows that H_{ext} diminishes the B-site hyperfine field /larger line intensity in the center of the spectrum/ and increases the A-site hyperfine field /smaller line intensity in the outer parts of the spectrum/. Taking into account that for the t = 1.9 sample $m_B > m_A$, it may be concluded that the signs of hyperfine fields at B and A sites are both negative. A distribution of the angles α'_A and α'_B has to be taken into account in order to get a satisfactory fit in Fig. 13.

Further Mössbauer effect investigations of $NiFe_{2-t}Al_tO_4$ series are in progress.

We would like to thank Dr. W. Zarek for providing us with the samples.

References:

1. G. Blasse, Philips Res. Repts. Suppl., 3, 1 /1964/.
2. E. De Grave, C. Dauve, A. Govaert and J. De Sitter, Appl. Phys., 12, 131 /1977/.
3. F. Van Der Woude and A. J. Dekker, phys. stat. sol., 9, 775 /1965/.
4. A. J. Dekker, in Hyperfine Interactions, edited by A. J. Freeman and R. B. Frankel /Academic Press, New York, 1967/, p. 679.
5. F. Van Der Woude, C. Blaauw and A. J. Dekker, Proc. Conf. Appl. Mössbauer Effect, Tihany, 1969, p. 133.
6. Y. Ishikawa, J. Appl. Phys., 35, 1054 /1964/.
7. H. Yamamoto, T. Okada, H. Watanabe and M. Fukase, J. Phys. Soc. Japan, 24, 275 /1968/.
8. F. Basile and P. Poix, phys. stat. sol., /a/ 35, 153 /1976/.
9. K. P. Belov, in Ferrity v silnych magnitnych polach, Izd. Nauka, Moskva, 1972, p. 63.
10. J. Piekoszewski, A. Konwicki, J. Suwalski, K. Kisyńska, A. Miracka and S. Makolagwa, Proc. Int. Conf. Mössbauer Spectr., Bucharest, 1977, Vol. 1, p. 163.
11. R. P. Frankel, in Mössbauer Effect Methodology, edited by I. J. Gruverman, C. W. Seidel and D. K. Dieterly /Plenum Press, New York and London, 1974/, Vol. 9, p. 151.
12. J. Chappert, J. de Physique, Colloq., 35, C6-71 /1974/.
13. J. J. Van Loef, Physica, 32, 2102 /1966/.
14. B. J. Evans, in Mössbauer Effect Methodology, edited by I. J. Gruverman /Plenum Press, New York, 1968/, Vol. 4, p. 139.

15. J. P. Morel, J. Phys. Chem. Solids, 28, 629 /1967/.
16. G. A. Sawatzky, F. Van Der Woude and A. H. Morrish, Phys. Rev., 187, 747 /1969/.
17. J. M. D. Coey and G. A. Sawatzky, phys. stat. sol., /b/ 44, 673 /1971/.
18. P. E. Clark and A. H. Morrish, phys. stat. sol., /a/ 12, 687 /1973/.
19. A. H. Morrish and P. E. Clark, Phys. Rev., B 11, 278 /1975/.
20. J. J. Bara, phys. stat. sol., /a/ 44, 737 /1977/.
21. J. J. Bara, A. T. Pędziwiatr, Z. M. Stadnik, A. Szytuła, J. Todorovič, Z. Tomkowicz and W. Zarek, phys. stat. sol., /a/ 44, 325 /1977/.
22. J. M. Daniels and A. Rosencwaig, Can. J. Phys., 48, 381 /1970/.
23. P. Raj and S. K. Kulshreshtha, phys. stat. sol., /a/ 4, 501 /1971/.
24. E. De Grave, R. Vanleerberghe, C. Dauve, J. De Sitter and A. Govaert, J. de Physique, Colloq., 37, C6-97 /1976/.
25. G. A. Petitt and D. W. Forester, Phys. Rev., B 4, 3912 /1971/.
26. C. M. Srivastava, S. N. Shringi and R. G. Srivastava, Phys. Rev., B 14, 2041 /1976/.
27. E. W. Gorter, Philips Res. Repts., 9, 295 /1954/.
28. Z. M. Stadnik and W. Zarek, phys. stat. sol., /b/ 91, K83 /1979/.
29. B. J. Evans and S. S. Hafner, J. Phys. Chem. Solids, 29, 1573 /1968/.
30. B. J. Evans and L. J. Swartzendruber, J. Appl. Phys., 42, 1628 /1971/.
31. L. K. Leung, B. J. Evans and A. H. Morrish, Phys. Rev., B 8, 29 /1973/.
32. G. A. Sawatzky and F. Van Der Woude, J. de Physique, Colloq., 35, C6-47 /1974/.
33. G. Czjzek and W. G. Berger, Phys. Rev., B 1, 957 /1970/.
34. S. Krupička, in Fizika ferritov i rodstvennych im okislov, Izd. Mir, Moskva, 1976.
35. J. Göring, W. Wurtinger and R. Link, J. Appl. Phys., 49, 269 /1978/.